Journal of Environmental Protection, 2014, 5, 1630-1640
Published Online December 2014 in SciRes. http://www.scirp.org/journal/jep
http://dx.doi.org/10.4236/jep.2014.517154

Scientific Research

Visible Light Photoelectrocatalytic Degradation of Rhodamine B Using Ti/TiO_2-NiO Photoanode

Sayekti Wahyuningsih, Candra Purnawan, Teguh Endah Saraswati, Edi Pramono, Ari Handono Ramelan, Setyo Pramono, Ari Wisnugroho

Inorganic Material Research Group, Department of Chemistry, Faculty Mathematics and Natural Science, Sebelas Maret University, Surakarta, Indonesia
Email: sayekti@mipa.uns.ac.id

Received 22 September 2014; revised 18 October 2014; accepted 12 November 2014

Abstract

The method of Ti/TiO_2-NiO photoelectrode prepared by using sol-gel method continued by calcination process was introduced. The prepared TiO_2-NiO film was observed with XRD and TEM. The anatase-rutile TiO_2 was mainly on the prepared TiO_2-NiO composite surface electrode. In addition to NiO, the composite also formed $NiTiO_3$ that increased with increasing calcination temperature. Photoelectrocatalytic degradation of Rhodamine B (RB) using this electrode was investigated, and anodic potential and pH were optimized. RB degradation was investigated under different conditions, and it showed that photoelectrocatalytic degradation could achieve efficient and complete mineralization of organic pollutant. Through comparison of the photoelectrocatalytic oxidation using the Ti/TiO_2-NiO electrode operated by single photoanode with the Ti/TiO_2-NiO electrode operated by several photoanode, it was found that the photoelectrocatalytic efficiency of that by series photoanodes was higher. Additionally, photoelectrocatalytic system was performed at the several different photoelectrodes, which verified the higher photocatalytic activity compared with the single photoelectrode.

Keywords

Ti/TiO_2-NiO Photoelectrode, Visible Light, Photoelectrocatalysis Degradation, Rhodamine B

1. Introduction

Titanium dioxide (TiO_2) was widely used in photocatalytic degradation of the organic pollutants that could not

How to cite this paper: Wahyuningsih, S., Purnawan, C., Saraswati, T.E., Pramono, E., Ramelan, A.H., Pramono, S. and Wisnugroho, A. (2014) Visible Light Photoelectrocatalytic Degradation of Rhodamine B Using Ti/TiO_2-NiO Photoanode. *Journal of Environmental Protection*, **5**, 1630-1640. http://dx.doi.org/10.4236/jep.2014.517154

be degraded easily such as dyes because of its favorable physical, chemical and photocatalytic properties and high stability [1]-[8]. This photocatalytic method was based on the reactive properties of photogenerated electron-hole pairs. They were generated in the semiconductor (TiO_2) particles under irradiation at suitable wavelengths ($\lambda \leq 400$ nm). These electrons and holes could also recombine. Since the hole was a powerful oxidizing agent, it could decompose contaminants adsorbed on the TiO_2 surface. Meanwhile, it could also oxidize water to produce hydroxyl radicals that could decompose organic pollutants in water [9]-[12]. There were many reports on photoelectrocatalytic degradation of organic pollutants by using TiO_2 electrodes which were prepared by coating the surfaces of electrically conducting sub-strates (ITO, Ti) with TiO_2 film. In this method, positive potential was applied on the working electrode (Ti/TiO_2 electrode), which could inhibit the recombination of electrons and holes and enhance the efficiency of photocatalytic degradation of organic compounds [5] [6] [13]-[18].

In order to improve the photoelectrocatalytic capability of TiO_2 film, preparation of TiO_2 film was extensively studied. TiO_2 films were often prepared by using either sol-gel method [19]-[25], pray pyrolysis [26] or sputtering [27]. Metal oxides, such as CuO, Cu_2O, Fe_2O_3, WO_3, MoO_3, ZnO, NiO, SnO_2, and so on, have been considered for band-gap engineering of TiO_2 as these oxides have compatible processing strategies with TiO_2 [28]-[37]. Among these oxides, low band-gap CuO or NiO is used as sensitizers to use visible radiation, whereas other large band-gap oxides (e.g., ZnO, SnO_2) are coupled with TiO_2 for extrinsic trapping of photogenerated charge carriers to enhance photoactivity. Among these, coupling TiO_2 with NiO still attracts less attention. The band gaps of SnO_2 and TiO_2 are 3.80 and 3.2 eV [38], respectively, and the CB edge of NiO is 0.5 V above that of TiO_2 [39]. When the two semiconductor particles are coupled, the CB of NiO acts as a sink for photogenerated electrons. Since the photogenerated holes move in the opposite direction, they accumulate in the VB of the TiO_2 particle, which increases the efficiency of charge separation.

In this paper, Ti/TiO_2-NiO electrode was prepared by using sol-gel method. The crystalline structure and surface morphology of TiO_2 film were evaluated by using X-ray diffraction (XRD) and TEM. The effect of crystalline size and structure was discussed. The photoelectrocatalytic ability of this electrode for degradation of Rhodamine B (RB) (**Figure 1**) and the effect of anodic potential and pH on this photoelectrocatalytic reaction were investigated. The photoelectrocatalytic oxidation using the Ti/TiO_2-NiO electrode calcinated by furnace was compared. Additionally, photoelectrocatalytic oxidation measurements were performed at the variously counter electrodes of Ti (commercial), Ti/TiO_2, which indicated the higher photocatalytic activity of the Ti/TiO_2 electrode further.

The mechanism of the RB photodegradation may include the following possible steps [40]:

$$\mathrm{RB} + \mathrm{O_2^{-\bullet}} \longrightarrow 2\ \text{rhodamine} \longrightarrow \text{products} \quad (1)$$

$$\mathrm{RB} + \mathrm{TiO_2(e^-)} \longrightarrow 2\ \text{rhodamine} \longrightarrow \text{products} \quad (2)$$

$$\mathrm{RB} + \mathrm{OH^{\bullet}} \longrightarrow \mathrm{RB^{+\bullet}} + \mathrm{OH^-} \quad (3)$$

$$\mathrm{RB^{+\bullet}} + \mathrm{O_2^{-\bullet}} \longrightarrow 2\ \text{rhodamine} \longrightarrow \text{products} \quad (4)$$

The cationic dye radical of RB is degraded into carbon dioxide, water, and mineral acids through a rhodamine intermediate. The rhodamine intermediate could be detected by UV-VIS spectroscopy from approximately 240 nm to 360 nm. In principle, the degradation process of RB decreases the absorption peak at 543 nm, but increases absorption peaks at approximately 240 - 360 nm. Qu *et al*. (1998) [28] reported that $OOH^{\bullet}$ and $OH^{\bullet}$ are necessary for the *N*-de-ethylation of RB, which, in turn, is necessary for complete degradation of the dye.

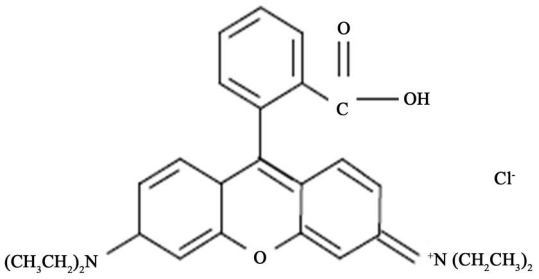

Figure 1. Structure of Rhodamine B.

2. Experiment

2.1. Reagent

Titanium (99.7%, in area 10 cm × 3 cm) was purchased from the Far East Ti Equipment Co., Shanghai, China. RB, titanium tetraisopropoxide (TTIP), ethanol, acetic acid, nickel chloride and other chemical reagents were purchased from E. Merck (Indonesia). All reagents were of analytical reagent grade quality. All solutions were prepared with doubly distilled water.

2.2. Device

X-ray data were collected by using a D8ADVANCE X-ray diffractometer (Bruker axs Co., Germany) based on CuKα radiation. The 2θ (two-theta) angle of the diffractometer was stepped from 10˚ to 80˚ by 0.03˚ increments. Transmission Electron microscope (TEM) was obtained by a JOEL JEM 1400 (Japan) with an in-column energy filter. Electrochemical experiments were performed with a Potentiostat (Jiangsu Electroanalytical Co., China). The two electrode system consisted of a Ti/TiO_2-NiO electrode as the working electrode, electrode and a Ti/TiO_2 as the counter electrode. The radiation source was a halogen lamp (300 W, Osram).

2.3. TiO_2 Film Preparation

The TiO_2 film has been synthesized by procedures that have been published previously [40]. A 10 mL solution of TTIP was hydrolysed in the 100 mL acetic acid glacial solution and mixed under vigorous stirring in an ice water-bath (10˚C - 15˚C) until a clear yellow solution of TiO_2 nanocrystals was formed. The solution was heated at 90˚C for 2 h when it became a gel, which was then placed in an oven at 150˚C for 24 h to undergo an aging process. Next, the TiO_2 xerogel was ground and pulverized into a fine powder and calcined in a muffle furnace at 400˚C for 2 h at a heating rate of 10˚C·min^{-1}. Then, ethanol was added to the TiO_2 powder before dip-coating to the Ti mesh. The TiO_2-coated Ti mesh was then dried at 100˚C for 5 min. The coating and drying treatments was repeated three times.

2.4. TiO_2-NiO Films Preparation

1.145 grams of synthesized xerogel TiO_2 (previous procedure) was added in 0.81 grams of $NiNO_3 \cdot 6H_2O$ that has dissolved in 25 ml of distilled water. The mixed solution was stirred with magnetic stirrer to fuse. Then, the uniform mixture was dried at 110˚C for 3 h. To improve the crystalline TiO_2-NiO after the green suspension was formed, it was calcinated at various temperature of 150˚C, 300˚C, 400˚C, 500˚C, 600˚C, and 700˚C for 4 hours at 10˚C/min. The crystalline TiO_2-NiO composite was superimposed onto a SnO_2F conductive glass and was dried at 110˚C for 3 h. The coating and drying treatments was repeated three times.

2.5. Photoelectrodegradation Experiment

In order to investigate the photoelectrocatalytic (PEC) activity of the prepared sensitized TiO_2 thin film, a series of degradation experiments of Rhodamine B in aqueous solutions were performed. The initial concentration of Rhodamine B was 5 mg·L^{-1}, with 0.05 mol·L^{-1} of NaCl used as the supporting electrolyte. The total volume of the solution was 10 mL. Experiments were carried out in an optical quality quartz cell equipped with a two-electrode system. A copper wire as well as Ti plate was used as the counter electrode. The front of the working electrode was irradiated with a 300 W visible light lamp (Halogen lamp, Osram) and the progress of the photoelectrocatalytic degradation was recorded at defined intervals by UV-VIS spectroscopy. The PEC degradation of RB was performed at voltages of 1.0 V to +10.0 V and at various pH values.

3. Results and Discussions

3.1. The Characteristics of TiO_2 Film

The TiO_2 films prepared by sol-gel from titanium tetraisopropoxide precursor were characterized by XRD, as shown in **Figure 2**. The present work, the sol-gel method was carried out under acidic conditions with acetic acid as solvent. The use of acetic acid as the solvent, as well as activating the formation of $Ti(OCOCH_3)(O^iPr)_2$ complexes, permits control of both the degree of condensation and the oligomerisation and induces preferential

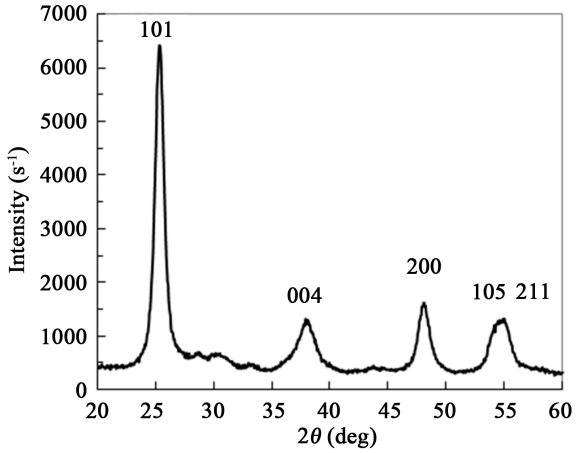

Figure 2. XRD pattern of prepared anatase TiO_2.

crystallisation of TiO_2 in the anatase phase. In the first case, a spherical and relatively monodisperse aggregates of nanocrystallites could be obtained. The growth kinetics of the aggregates is determined by the stability of the colloid. The TiO_2 particles formed are relatively stable and a white suspension is gradually formed due to the precipitation of large aggregates.

However, under the acetic acid conditions using the $Ti(O^iPr)_4$ precursor, the complexes formation was occur as described in the equation below [40].

$$CH_3COO^- + Ti(O^i\,Pr)_4 \xrightarrow{H^+} Ti(OCOCH_3)(O^i\,Pr)_2$$

In further hydrolysis and condensation steps, the $Ti(OCOCH_3)(O^iPr)_2$ product will produce nanotitania. In this research, nano-TiO_2 was prepared from stock solutions of 110 mL solution containing titanium tetraisopropoxide and acetic acid solution in a volume ratio of 1:10 in a water bath (10˚C - 15˚C). The anatase of TiO_2 was obtained after an annealing process at 400˚C (annealing rate of 10˚C min). **Figure 2** shows that the XRD pattern of the TiO_2 thus prepared exhibits strong diffraction peaks at $2\theta = 25.35^\circ$ ($d_{101} = 3.51$ Å), $2\theta = 37.90^\circ$ ($d_{004} = 2.37$ Å), $2\theta = 48.11^\circ$ ($d_{200} = 1.89$ Å), $2\theta = 54.16^\circ$ ($d_{105} = 1.69$ Å), and $2\theta = 54.96^\circ$ ($d_{211} = 1.67$ Å), indicating that TiO_2 is formed by the anatase phase. All peaks are in good agreement with the standard spectrum (JCPDS No.: JCPDS # 782-484). This result suggested that the nano-TiO_2 powder was irregularly polycrystalline. The XDR pattern shows that only the anatase phase is formed.

In addition, TEM was used to further examine the crystallite/particle size, crystallinity, and morphology of the samples. Clear spherical and non-homogeneous structures can be seen in **Figure 3(a)**, with the average size of the primary particle approximately 10 nm, which is in good agreement with the value determined by XRD. The particle of TiO_2 in the anatase phase has a mostly spherical morphology (**Figure 2(a)**). The area selected for electron diffraction pattern analysis (SAED), confirming that the TiO_2 nanoparticles are highly crystalline in the anatase phase, in good agreement with the standard JCPDS # 782-484 and XRD result.

3.2. The Characteristics of TiO_2-NiO Film

The composite of TiO_2-NiO was obtained after an annealing process at 700˚C (annealing rate of 10˚C min). **Figure 4** shows that the XRD pattern of the TiO_2-NiO thus prepared exhibits strong diffraction peaks at $2\theta = 27.45^\circ$ ($d_{110} = 3.2452$ Å), $2\theta = 36.10^\circ$ ($d_{101} = 2.4849$ Å), $2\theta = 39.20^\circ$ ($d_{200} = 2.2952$ Å), $2\theta = 41.25^\circ$ ($d_{111} = 2.1858$ Å), $2\theta = 44.05^\circ$ ($d_{210} = 2.0531$ Å), $2\theta = 54.36^\circ$ ($d_{211} = 1.6858$), and $2\theta = 56.66^\circ$ ($d_{220} = 1.6227$ Å) which are the characterization of rutile TiO_2 according to the standard JCPDS No. 870-710. There are also several peaks indicates the anatase phase at $2\theta = 25.40^\circ$ ($d_{101} = 3.5023$ Å), $2\theta = 37.90^\circ$ ($d_{004} = 2.3709$ Å), and $2\theta = 48.15^\circ$ ($d_{200} = 1.8874$ Å) according to the standard JCPDS No. 782-486. Peaks characteristic of $NiTiO_3$ are peaks at the $2\theta = 24^\circ$ ($d_{012} = 3.6584$ Å), $2\theta = 33^\circ$ ($d_{110} = 2.6911$ Å), $2\theta = 49^\circ$ ($d_{024} = 1.8356$ Å), and $2\theta = 57^\circ$ ($d_{018} = 1.5969$ Å). All peaks are in good agreement with the standard spectrums JCPDS No. 753-757.

TEM was used to further examine the crystallite/particle size, and morphology of the TiO_2-NiO composites samples. Clear spherical and non-homogeneous structures can be seen in **Figure 5(a)**, with the average size of

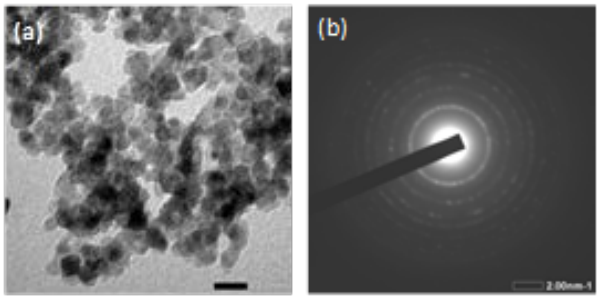

Figure 3. Images of anatase phase. (a) TEM image of nano-TiO_2 powder; (b) SAED pattern of nano-TiO_2 powde.

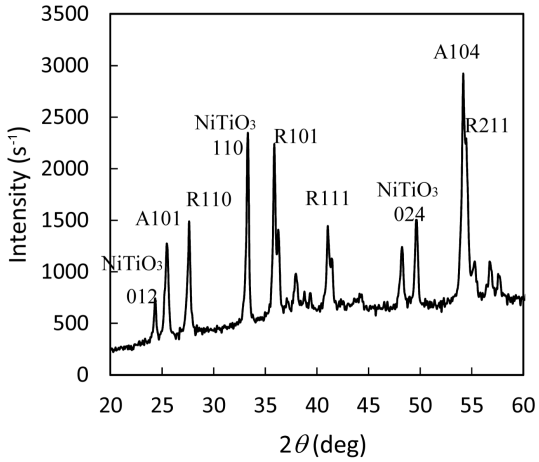

Figure 4. XRD pattern of TiO_2-NiO thin film.

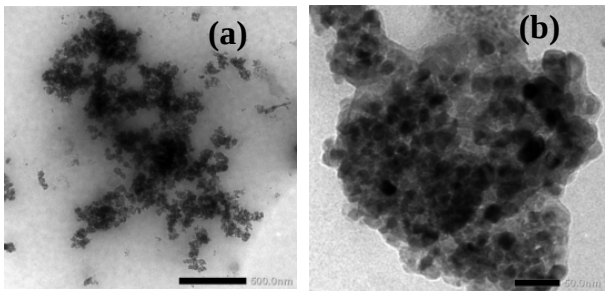

Figure 5. TEM Image of TiO_2-NiO nanoparticle were used for photoanode preparation (a) 500 nm bar; (b) 50 nm bar.

the primary particle approximately 20 - 30 nm, which is in good agreement with the value determined by XRD. The particle of TiO_2 in the anatase phase has a mostly spherical morphology (**Figure 5(a)**). The area selected for electron diffraction pattern analysis (SAED) (**Figure 5(b)**), confirming that the TiO_2-NiO nanoparticles are also highly crystalline in the anatase phase, rutile phase and $TiNiO_3$.

While the part of photoanoda TiO_2-NiO composite shows that TiO_2-NiO materials were deposited on the Ti contained on porous amorphous silica (**Figure 6**). The conductivity character of those composite is shown in **Figure 7**. The profile shows that the composite photoanoda Ti/TiO_2-NiO quite well as electron generation. Based on the bar graph in **Figure 8**, that shows the percentage of formation of NiO in a variety of temperatures, as well as the byproducts $NiTiO_3$. $NiTiO_3$ arises due to the formation of NiO and TiO_2. Percentage of NiO in the composite achieving optimum condition at 500˚C reached 22.78%. Another product is a composite of $NiTiO_3$ that appears on composite roasted at 600˚C and roasted at 700˚C composite. Increased temperature and addition of NiO dopants were affecting the TiO_2 crystalization. Increased temperature and the addition of NiO dopants

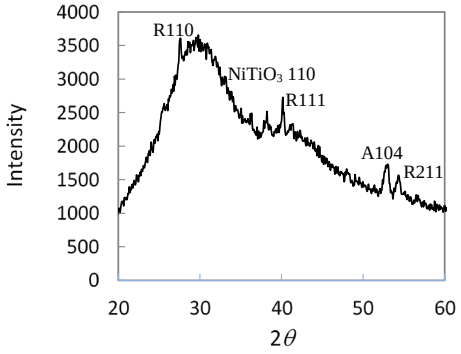

Figure 6. XRD Pattern of Ti/TiO_2-NiO electrode material.

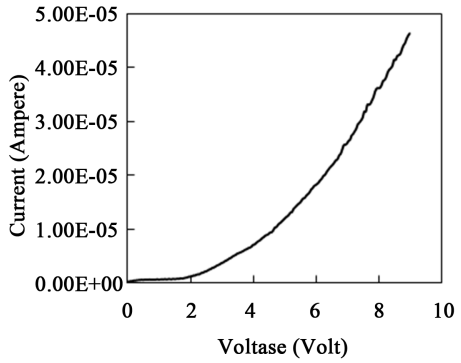

Figure 7. Voltage applied-current profile of the Ti/TiO_2-NiO electrode. Counter electrode: Ti/TiO_2 electrode.

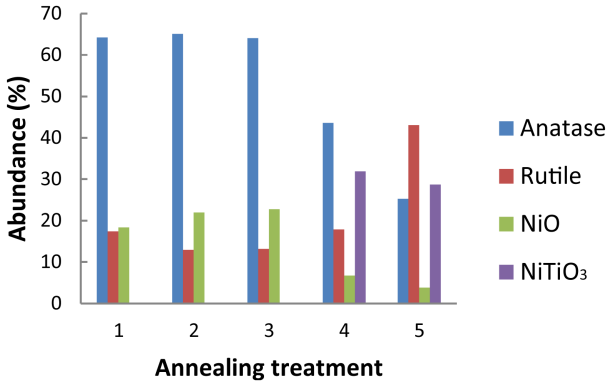

Figure 8. Relative abundance of anatase phase, rutile phase, NiO, and $NiTiO_3$ on TiO_2-NiO composite result of annealing at 300˚C (1), 400˚C (2), 500˚C (3), 600˚C (4), and 700˚C (5).

were affecting TiO_2 crystal structure transformation. The addition of these dopants was found to suppress the transformation of anatase into rutile (compared with no addition of dopand, **Table 1**). The occurrence of these structural transformations will change the photoactivity of TiO_2 and further explained in TiO_2-NiO composite activity for photodegradation of Rhodamine B.

3.3. Influence of pH

This experiment was carried out at different pH values of 2.0, 4.0, 6.0, 8.0 and 10.0, respectively, in order to investigate the process of RB photoelectrocatalytic degradation. The experimental results were shown in **Figure 9**. It demonstrated that the efficiency of the photoelectrode on the photoelectrocatalytic degradation of RB was

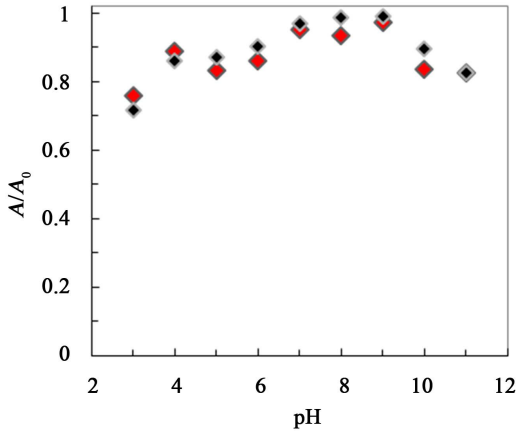

Figure 9. Absorbance of RB solution after photoelectrocatalytic degradation for 180 min at various pH values under visible light irradiation ([NaCl] = 0.05 M, [RB] = 5×10^{-4} mass%, applied bias potential 1.0 V).

Table 1. Anatase to rutile ratio (A/R) of the synthesized TiO_2 and composite TiO_2-NiO.

A/R ratio	Annealing temperature					
	150˚C	300˚C	400˚C	500˚C	600˚C	700˚C
TiO_2	1:0	1:0	1:0	1:0.06	1:0.72	1:9.93
TiO_2-NiO composite	1:0	1:0.20	1:0.20	1:0.21	1:0.41	1:1.70

improved with the increase in pH value and the rate constant of the photoelectrocatalytic degradation of RB was also increased at the same time. The results showed that the photoelectrocatalytic activity of the photoelectrode was increased due to the increase in pH value. The study of the effect of pH value on the efficiency of photoelectrocatalytic degradation of organic dye was valuable but complicated. Firstly, pH value had significant effect on the absorption behavior of the organic dye on the catalyst surface. The point of zero charge of the TiO_2 that was the catalyst was at pH 6.4. Thus, the TiO_2 surface was positively charged in the media with pH less than 6.4, whereas it was negatively charged under the conditions with the pH greater than 6.4. The value of pH could also influence the charge carried by the molecule [40], the molecule of RB was cationic form at lower than 4. When the pH value was less on the catalyst surface became difficult because of an electrostatic repulsive force. When the pH value was greater than 4, the molecule of RB was in the zwitterionic form and a certain part of the molecule was attracted by the catalyst surface due to the electrostatic attraction [16]. As a result, the efficiency of the photoelectrocatalytic degradation of RB was relatively low with the pH less than 4 while the efficiency was increased with the pH greater than 4. Secondly, the change of pH had an important effect on modifying the position of the TiO_2 conduction band (60 mV per pH unit) [35]. Thus, the oxidizing ability of photogenerated holes was raised, *i.e.* the hydroxyl radical production was facilitated in the oxidation of water (or hydroxide ions) by photogenerated holes. The more alkaline, the more readily water (or hydroxide ions) underwent oxidation to generate hydroxyl radicals on the catalyst surface. Therefore, the photoelectrocatalytic degradation of RB was more efficient due to the increase in pH value. The pH value of 10 was selected in subsequent experiments.

3.4. Degradation of RB under Different Applied Potential Bias Conditions by the Proposed Photoelectrode

When the potential was 3.0 V, the rate of photoelectron transport process was lower and controlled the overall PEC oxidation. Thus, the photocurrent increased within the potential of 3.0 - 5.0 V. Once the applied bias exceeded 5.0 V, the interfacial oxidation, which was slower than the photoelectron transport, became the rate-determining step of the overall process. Under this condition the photocurrent saturated gradually. The anodic potential was an important parameter in the process of photoelectrocatalytic degradation of RB. The effect of applied potential was determined by using a series of potentials. To study the key factors affecting the photodegradation of RB, a series of tests were executed under different experimental conditions in which the deduction

of Vis absorbance was estimated.

After 5 min degradation (batch system), about 96.3% of RB was removed. Photoelectrocatalytic (PEC) experiment 1 was carried out under halogen lamp irradiation using the Ti/TiO_2-NiO photoelectrode with a potential voltage of +10.0 V. It was obvious that the degradation rate was very fast. But their applied potential voltages make the electrode surface damage rapidly. Furthermore, the continuous systems were done with applied potential bias of 4, 5, and 6 volts. The results are shown in **Table 2**. However, RB could not undergo complete degradation to produce CO_2 and H_2O, as a result, the intermediates were produced during the process [40]. Therefore, PEC method showed high complete mineralization activity in the RB degradation reaction. **Figure 10** shows no prominent peak in the UV region around 370 nm as an indication of an intermediate peak of rhodamine.

3.5. Compared the Photoelectrocatalytic Oxidation Using Several Photoelectrodes

Compared the photoelectrocatalytic oxidation using the Ti/TiO_2 electrode by batch system as well as by single photoanode (**Table 2**), the photoelectrocatalytic oxidation process using integrated photoanode can enhance the RB degradation, respectively, as shown in **Table 3**. The experimental results also demonstrated that the reaction rate of RB degradation using several electrode by continuous system was higher than that by single photoanode.

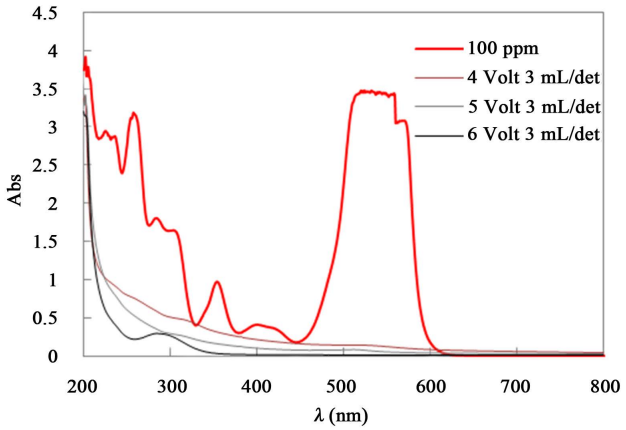

Figure 10. Electronic spectra of Rhodamine B before and after photoelectrocatalytic degradation process at a variation applied voltage.

Table 2. Degradation of RB (%) under different experimental conditions using Ti/TiO_2-NiO photoanode with a 300 watts halogen lamp irradiation.

Experiment	Potential voltage of photoanode (volt)	Batch system (%)	Continuous system (%)	
			3 mL/sec	6 mL/sec
1	10	96.3*		
2	4		10.0	14.9
3	5		12.7	15.3
4	6		15.9	16.3

Table 3. Degradation of RB (%) under different experimental conditions using several photoanode of Ti/TiO_2-NiO, Ti/TiO_2-PbO, Ti/Ta-Ir and Ti/Ru-Ir photoanodes, respectively, under a 300 watts halogen lamp irradiation.

Applied bias potential of photoanode (volt)	Flow rate	
	3 mL/sec	6 mL/sec
4	98.0	95.5
5	99.3	97.0
6	99.6	98.0

4. Conclusion

In this paper, the method of preparation Ti/TiO_2 photoelectrode was firstly presented. The anatase TiO_2 was mainly on the prepared electrode surface. Photoanode of the TiO_2-NiO composite synthesized by sol-gel method showed that the photoelectrocatalytic degradation ran very well. Photoelectrocatalytic degradation of RB using this electrode was investigated, and the operating conditions were optimized. pH and applied bias voltage affected the rate of photoelectrocatalytic degradation of Rhodamine B. By the comparison of the photoelectrocatalytic oxidation using the Ti/TiO_2 NiO electrode operated by single photoanode and the TiO_2 NiO electrode operated by several photoanode, it was found that the photoelectrocatalytic efficiency of that by series photoanodes was higher. Additionally, photoelectrocatalytic system was performed at the several different photoelectrodes, which verified the higher photocatalytic activity of the single system-treated electrode further.

Acknowledgements

This work is supported by the STRANAS research program (Contract Number No. 6562/UN27.16/PN/2014) from Director of Higher Education Ministry of Education and Culture of Indonesia.

References

[1] Krýsa, J., Keppert, M., Waldner, G. and Jirkovský, J. (2005) Immobilized Particulate TiO_2 Photocatalysts for Degradation of Organic Pollutants: Effect of Layer Thickness. *Electrochimica Acta*, **50**, 5255-5260. http://dx.doi.org/10.1016/j.electacta.2005.01.054

[2] Usui, H., Miyamoto, O., Nomiyama, T., Horie, Y. and Miyazaki, T. (2005) Photo-Rechargeability of TiO_2 Film Electrodes Prepared by Pulsed Laser Deposition. *Solar Energy Materials and Solar Cells*, **86**, 123. http://dx.doi.org/10.1016/j.solmat.2004.06.006

[3] Irmak, S., Kusvuran, E. and Erbatur, O. (2004) Degradation of 4-Chloro-2-Methylphenol in Aqueous Solution by UV Irradiation in the Presence of Titanium Dioxide. *Applied Catalysis B*: *Environmental*, **54**, 85. http://dx.doi.org/10.1016/j.apcatb.2004.06.003

[4] Vinodgopal, K., Hotchandani, S. and Kamat, P.V. (1993) Electrochemically Assisted Photocatalysis: Titania Particulate Film Electrodes for Photocatalytic Degradation of 4-Chlorophenol. *Journal of Physical Chemistry*, **97**, 9040. http://dx.doi.org/10.1021/j100137a033

[5] Osugi, M.E., Umbuzeiro, G.A., Anderson, M.A. and Zanoni, M.V.B. (2005) Degradation of Metallophtalocyanine Dye by Combined Processes of Electrochemistry and Photoelectrochemistry. *Electrochimica Acta*, **50**, 5261. http://dx.doi.org/10.1016/j.electacta.2005.01.058

[6] Leng, W.H., Zhang, Z. and Zhang, J.Q. (2003) Photoelectrocatalytic Degradation of Aniline over Rutile TiO_2/Ti Electrode Thermally Formed at 600˚C. *Journal of Molecular Catalysis A*: *Chemical*, **206**, 239. http://dx.doi.org/10.1016/S1381-1169(03)00373-X

[7] Ma, Y. and Yao, J.N. (1999) Comparison of Photodegradative Rate of Rhodamine B Assisted by Two Kinds of TiO_2 Films. *Chemosphere*, **38**, 2407. http://dx.doi.org/10.1016/S0045-6535(98)00434-2

[8] Wu, J.-M. and Zhang, T.-W. (2004) Photodegradation of Rhodamine B in Water Assisted by Titania Films Prepared through a Novel Procedure. *Journal of Photochemistry and Photobiology A*: *Chemistry*, **162**, 171. http://dx.doi.org/10.1016/S1010-6030(03)00345-9

[9] Ishikawa, Y. and Matsumoto, Y. (2001) Electrodeposition of TiO_2 Photocatalyst into Nano-Pores of Hard Alumite. *Electrochimica Acta*, **46**, 2819. http://dx.doi.org/10.1016/S0013-4686(01)00490-X

[10] Kim, D.H. and Anderson, M.A. (1994) Photoelectrocatalytic Degradation of Formic Acid Using a Porous Titanium Dioxide Thin-Film Electrode. *Environmental Science & Technology*, **28**, 479. http://dx.doi.org/10.1021/es00052a021

[11] Konstantinou, I.K. and Albanis, T.A. (2004) TiO_2-Assisted Photocatalytic Degradation of Azo Dyes in Aqueous Solution: Kinetic and Mechanistic Investigations. *Applied Catalysis B*: *Environmental*, **49**, 1-14. http://dx.doi.org/10.1016/j.apcatb.2003.11.010

[12] Palombaria, R., Ranchellaa, M., Rola, C. and Sebastiani, G.V. (2002) Oxidative Photoelectrochemical Technology with Ti/TiO_2 Anodes. *Solar Energy Materials and Solar Cells*, **71**, 359-368. http://dx.doi.org/10.1016/S0927-0248(01)00093-9

[13] Christensen, P.A., Curtis, T.P., Egerton, T.A., Kosa, S.A.M. and Tinlin, J.R. (2003) Photoelectrocatalytic and Photocatalytic Disinfection of *E. coli* Suspensions by Titanium Dioxide. *Applied Catalysis B*: *Environmental*, **41**, 371-386. http://dx.doi.org/10.1016/S0926-3373(02)00172-8

[14] Li, X.Z., Li, F.B., Fan, C.M. and Sun, Y.P. (2002) Photoelectrocatalytic Degradation of Humic Acid in Aqueous

Solution Using a Ti/TiO_2 Mesh Photoelectrode. *Water Research*, **36**, 2215-2224. http://dx.doi.org/10.1016/S0043-1354(01)00440-7

[15] Jiang, D., Zhao, H., Zhang, S. and John, R. (2004) Kinetic Study of Photocatalytic Oxidation of Adsorbed Carboxylic Acids at TiO_2 Porous Films by Photoelectrolysis. *Journal of Catalysis*, **223**, 212-220. http://dx.doi.org/10.1016/j.jcat.2004.01.030

[16] Guo, Y., Zhao, J., Zhang, H., Yang, S., Qi, J., Wang, Z. and Xu, H. (2005) Use of Rice Husk-Based Porous Carbon for Adsorption of Rhodamine B from Aqueous Solutions. *Dyes and Pigments*, **66**, 123-128. http://dx.doi.org/10.1016/j.dyepig.2004.09.014

[17] Chen, J., Liu, M., Zhang, L., Zhang, J. and Jin, L. (2003) Application of Nano TiO_2 towards Polluted Water Treatment Combined with Electro-Photochemical Method. *Water Research*, **37**, 3815-3820. http://dx.doi.org/10.1016/S0043-1354(03)00332-4

[18] Butterfield, I.M., Christensen, P.A., Curtis, T.P. and Gunlazuardi, J. (1997) Water Disinfection Using an Immobilised Titanium Dioxide Film in a Photochemical Reactor with Electric Field Enhancement. *Water Research*, **31**, 675-677. http://dx.doi.org/10.1016/S0043-1354(96)00391-0

[19] Nazeeruddin, M.K., Kay, A., Rodicio, I., Humphry-Baker, R., Muller, E., Liska, P., Vlachopoulos, N. and Gratzel, M. (1993) Conversion of Light to Electricity by Cis-X2bis(2,2'-bipyridyl-4,4'-dicarboxylate)ruthenium(II) Charge-Transfer Sensitizers (X = Cl-, Br-, I-, CN-, and SCN-) on Nanocrystalline Titanium Dioxide Electrodes. *Journal of the American Chemical Society*, **115**, 6382-6390. http://dx.doi.org/10.1021/ja00067a063

[20] Xu, Q. and Anderson, M.A. (1991) Synthesis of Porosity Controlled Ceramic Membranes. *Journal of Materials Research*, **6**, 1073-1081. http://dx.doi.org/10.1557/JMR.1991.1073

[21] Trapalis, C.C., Karakassides, M.A., Kordas, G. and Aslanoglou, X. (1995) Study of a Multilayer Wavelength-Selective Reflector Prepared by the Sol-Gel Process. *Materials Letters*, **25**, 265-269. http://dx.doi.org/10.1016/0167-577X(95)00183-2

[22] Dekany, I., Turi, L. and Kiraly, Z. (1999) CdS, TiO_2 and Pd° Nanoparticles Growing in the Interlamellar Space of Montmorillonite in Binary Liquids. *Applied Clay Science*, **15**, 221-239. http://dx.doi.org/10.1016/S0169-1317(99)00016-2

[23] Kim, D.J., Oh, S.H. and Kim, E.J. (2002) Influence of Calcination Temperature on Structural and Optical Properties of TiO_2 Thin Films Prepared by Sol-Gel Dip Coating. *Materials Letters*, **57**, 355-360. http://dx.doi.org/10.1016/S0167-577X(02)00790-5

[24] Mogyorosi, K., Dekany, I. and Fendler, J.H. (2003) Preparation and Characterization of Clay Mineral Intercalated Titanium Dioxide Nanoparticles. *Langmuir*, **19**, 2938-2946. http://dx.doi.org/10.1021/la025969a

[25] Li, J., Li, L., Zheng, L., Xian, Y. and Jin, L. (2006) Determination of Chemical Oxygen Demand Values by a Photocatalytic Oxidation Method Using Nano-TiO_2 Film on Quartz. *Talanta*, **68**, 765-770. http://dx.doi.org/10.1016/j.talanta.2005.06.012

[26] Golego, N., Studenikin, S.A. and Cocivera, M. (1999) Spray Pyrolysis Preparation of Porous Polycrystalline Thin Films of Titanium Dioxide Containing Li and Nb. *Journal of Materials Research*, **14**, 698-707. http://dx.doi.org/10.1557/JMR.1999.0095

[27] Lee, C.E., Atkins, R.A. and Taylor, H.F. (1987) Reflectively Tapped Optical Fibre Transversal Filters. *Electronics Letters*, **23**, 596-598. http://dx.doi.org/10.1049/el:19870428

[28] Qu, P., Zhao, J.C., Shen, T. and Hidaka, H. (1998) TiO_2-Assisted Photodegradation of Dyes: A Study of Two 2 Competitive Primary Processes in the Degradation of RB in an Aqueous TiO_2 Colloidal Solution. *Journal of Molecular Catalysis A*: *Chemical*, **129**, 257-268. http://dx.doi.org/10.1016/S1381-1169(97)00185-4

[29] Papp, J., Soled, S., Dwight, K. and Wold, A. (1994) Surface Acidity and Photocatalytic Activity of TiO_2, WO_3/TiO_2, and MoO_3/TiO_2 Photocatalysts. *Chemistry of Materials*, **6**, 496-500. http://dx.doi.org/10.1021/cm00040a026

[30] Liao, D.L., Badour, C.A. and Liao, B.Q. (2008) Preparation of Nanosized TiO_2/ZnO Composite Catalyst and Its Photocatalytic Activity for Degradation of Methyl Orange. *Journal of Photochemistry and Photobiology A*: *Chemistry*, **194**, 11-19. http://dx.doi.org/10.1016/j.jphotochem.2007.07.008

[31] Kansal, S.K., Singh, M. and Sud, D. (2008) Studies on TiO_2/ZnO Photocatalysed Degradation of Lignin. *Journal of Hazardous Materials*, **153**, 412-417. http://dx.doi.org/10.1016/j.jhazmat.2007.08.091

[32] Jiang, Y., Sun, Y., Liu, H., Zhu, F. and Yin, H. (2008) Solar Photocatalytic Decolorization of C.I. Basic Blue 41 in an Aqueous Suspension of TiO_2-ZnO. *Dyes Pigments*, **78**, 77-83. http://dx.doi.org/10.1016/j.dyepig.2007.10.009

[33] Tada, H., Hattori, A., Tokihisa, Y., Imai, K., Tohge, N. and Ito, S. (2000) A Patterned-TiO_2/SnO_2 Bilayer Type Photocatalyst. *The Journal of Physical Chemistry B*, **104**, 4585-4587. http://dx.doi.org/10.1021/jp000049r

[34] Liu, Z., Sun, D.D., Guo, P. and Leckie, J.O. (2007) An Efficient Bicomponent TiO_2/SnO_2 Nanofiber Photocatalyst Fabricated by Electrospinning with a Side-by-Side Dual Spinneret Method. *Nano Letters*, **7**, 1081-1085.

http://dx.doi.org/10.1021/nl061898e

[35] Kavan, L., Stoto, T., Gratzel, M., Fitzmaurice, D. and Shklover, V. (1993) Quantum Size Effects in Nanocrystalline Semiconducting Titania Layers Prepared by Anodic Oxidative Hydrolysis of Titanium Trichloride. *Journal of Physical Chemistry*, **97**, 9493-9498. http://dx.doi.org/10.1021/j100139a038

[36] Lin, C.F., Wu, C.H. and Onn, Z.N. (2008) Degradation of 4-Chlorophenol in TiO_2, WO_3, SnO_2, TiO_2/WO_3 and TiO_2/SnO_2 systems. *Journal of Hazardous Materials*, **154**, 1033-1039. http://dx.doi.org/10.1016/j.jhazmat.2007.11.010

[37] Sreetawang, T., Suzuki, Y. and Yoshikawa, S. (2005) Photocatalytic Evolution of Hydrogen over Mesoporous TiO_2 Supported NiO Photocatalyst Prepared by Single-Step Sol-Gel Process with Surfactant Template. *International Journal of Hydrogen Energy*, **30**, 1053-1062. http://dx.doi.org/10.1016/j.ijhydene.2004.09.007

[38] Inoue, T., Akira, F., Satoshi, K. and Kenichi, H. (1979) Photoelectrocatalytic Reduction of Carbon Dioxide in Aqueous Suspensions of Semiconductor Powders. *Nature*, **277**, 637-638. http://dx.doi.org/10.1038/277637a0

[39] Zhou, H., Qu, Y., Zeid, T. and Duan, X. (2012) Towards Highly Efficient Photocatalysts Using Semiconductor Nanoarchitectures. *Energy & Environmental Science*, **5**, 6732-6743. http://dx.doi.org/10.1039/c2ee03447f

[40] Wahyuningsih, S., Purnawan, C., Saraswati, T.E., Kartikasari, P.A. and Praistia, N. (2014) Visible Light Photoelectrocatalytic Degradation of Rhodamine B Using a Dye-Sensitised TiO_2 Electrode. *Chemical Papers*, **68**, 1248-1256. http://dx.doi.org/10.2478/s11696-013-0476-8